CHIN. PHYS. LETT. Vol. 38, No. 12 (2021) 123201

An Alternative Operation Scheme to Improve the Efficiency of a Stark Decelerator

Mei Du(杜美), Dongdong Zhang(张栋栋)*, and Dajun Ding(丁大军)*

Institute of Atomic and Molecular Physics, Jilin University, Changchun 130012, China

(Received 25 September 2021; accepted 2 November 2021; published online 18 November 2021)

A Stark decelerator can slow down polar molecules to very low velocities. When the velocities are very low, the number of cold molecules obtained is very small. In order to obtain a higher quantity of cold molecules, inspired by the work of Reens *et al.* [Phys. Rev. Res. 2 (2020) 033095], we propose an alternative method of operating a Stark decelerator. Through the trajectory simulation of OH molecules in the decelerator, we find that the number of cold molecules can be greatly increased by one order of magnitude at both low and high final velocities on a Stark decelerator consisting of around 150 electrodes. This development is due to the improved longitudinal and the transverse focusing property provided by the new switching schemes and the high-voltage configurations on the decelerator unit.

DOI: 10.1088/0256-307X/38/12/123201

When the temperatures of the molecular system decreases, the de Broglie wavelength of the molecule increases. In this case, quantum effects start playing an important role, i.e., molecules cannot be described by classical particle models.[1,2] On the other hand, low temperatures achieved in molecular assembles permit high precision measurements of fundamental properties of molecules, which is now a research frontier with the aim to discover new physics.[3–6] Moreover, proposals of using cold molecules as qubits to perform quantum computing emerge recently.[7,8] Motivated by these fascinating goals, cooling molecules down to various final temperatures has become an ever fast growing research field coined as cold molecules.

In the course of the study of cold molecular physics, the primary goal is to produce dense molecules with low temperatures. The cooling of molecules is much more difficult than the cooling of atoms which benefits from the laser cooling method as a working horse.[9–14] To achieve laser cooling, a closed cycle of absorption and emission is required, which is rare in molecules possessing complicated energy level structures. However, rich internal structures make molecules more interesting, to some extend, compared to atoms, e.g., the rotational and vibration transitions unique to molecules have the potential to boost the accuracy for the measurement of the temporal stability of fundamental constants.[15] A variety of methods have been developed to cool molecules down. We can roughly categorize these methods as direct cooling and indirect cooling. Direct cooling refers to cooling of chemically stable hot molecules through interactions with external fields. These include electric field Stark decelerators,[16–22] magnetic field Zeeman decelerators,[23–29] buffer gas cooling,[30,31] and direct laser cooling.[32–34] Indirect cooling refers to the process from cold atoms captured by lasers as the starting point, and then forming cold molecules through the association of them, such as optical association,[35,36] Feshbach resonance association,[37–40] and coherent synthesis.[41] Now, some molecules have been cooled by the above-mentioned methods. For example, CaF molecules have been laser cooled to 20 μK and loaded to an optical trap.[42] The optical association and magnetic-Feshbach resonance[43] remain the most efficient tools to generate ultra-cold molecules. Both of these methods can obtain molecular samples with temperatures below 1 mK. However, the fact that optical association and magnetic-Feshbach resonance technologies can only produce molecule out of alkali-metal atoms[44] limits their attractiveness to the chemistry community. The research on cold molecules in chemistry calls for more general molecular species. This study focuses on the Stark deceleration technique, which is considered as a general method to produce cold molecules. It is specially suitable for radicals. Currently, using Stark deceleration can reach temperatures to dozens of mK, however the density of the decelerated sample is still low. In this contribution, we explore the possibility of obtaining more molecules in a conventional Stark decelerator consisting of 150 pairs of electrodes to widen the applicability of this technique.

A Stark decelerator takes advantage of the Stark effect of polar molecules (or Rydberg atoms possessing large dipole moments). In a Stark decelerator, a narrow pulse of molecules is slowed by rapidly controlled inhomogeneous electric fields.[18,19,45] Be-

Supported by the National Key R&D Program of China (Grant No. 2019YFA0307701), the Science Challenge Project (Grant No. TZ2018005), and Jilin University.

*Corresponding authors. Email: dongdongzhang@jlu.edu.cn; dajund@jlu.edu.cn

© 2021 Chinese Physical Society and IOP Publishing Ltd

fore the molecules exit the high-field strength region, the field is switched to another configuration. The net effect is to remove the kinetic energies from the molecule, converting it to Stark energies and then returning the molecules to the same initial potential energy condition with no applied field. This process is repeated with successive stages of electrodes until the molecules have been slowed to the desired velocities.

Although a Stark decelerator can reduce the molecular velocity to a very low level, as the molecular velocity gradually decreases the number of molecules becomes smaller. There are several distinct mechanisms responsible for the loss of molecules during the deceleration process. One is inherent to the working principle. Stark deceleration relies on conservative forces. As being decelerated, the molecules feel the combined trapping potential formed by the decelerator and the deceleration in the moving frame. The effective trapping depth in the moving frame decreases as the deceleration increases.[45−48] The other mechanisms are related to the non-ideal transverse focusing force in a Stark decelerator and the longitudinal and transverse motional coupling.[49−52] In order to reduce the loss of molecules different operation schemes have been proposed, such as operating in the so-called $s = 3$ mode.[50] In this scheme the high-voltage configuration is changed every three pairs of electrodes, so that the molecules experience more stronger transverse force and thus are better focused. The disadvantage is that this method requires a three-times longer decelerator to slow molecules down to the same final speed compared to the ordinary switching operation scheme. The so-called advanced switching scheme[51] operates a Stark decelerator with ordinary length by switching the voltage configuration three times per deceleration stage. It offers the possibility to optimize the transverse focusing force by optimizing the timing of the high-voltage configuration switching and thus partially solves the over-focusing problem raised in the $s = 3$ mode. This scheme increases the number of molecules with final velocities from 150 m/s to 30 m/s by a factor of 2 compared to the normal operation scheme. In the recently proposed alternating switching scheme,[52] the high-voltage configuration of the decelerator is switched among three grounding electrode pairs, one with positive high voltage, and two positive and two grounding electrodes. This proposal has been simulated and tested on a decelerator with the length about 2 m. A factor of 4 in improvement is confirmed both experimentally and theoretically with the so-called F operation mode. Further improvement is indicated based on the trajectory simulation with the SF mode.

Complimentary to these existing methods and inspired by the work of Reens *et al.*,[52] we propose a novel switch sequence and high-voltage configurations for a Stark decelerator to mitigate the loss without lengthening the Stark decelerator. With the help of the 3D trajectory simulation, which has been proven to be able to reproduce experimental results accurately and guide the design of decelerators,[19,47−49,51,53−56] we demonstrate that (with the test molecule OH) the deceleration efficiency of the proposed new switching sequence (pm + normal) is more than one order of magnitude higher than the normal operation scheme. The deceleration efficiency of the pm + normal mode is a factor of 3 higher than that of the pg + normal mode (that is, SF mode proposed in Ref. [52]) on a shorter Stark decelerator (with 150 pairs of electrodes).

Theoretical Method. To simulate the trajectories of molecules in a Stark decelerator we first define a single molecule called synchronous molecule for which the initial and final velocity are predefined to get the timings for switching the high voltage configurations on the electrodes. Then we use these calculated timings to run trajectories for a bunch of molecules, which mimic the real experimental conditions. The amount of the kinetic energy a molecule loses at each stage depends on its position in the decelerator when the high voltage configuration of the electrodes is switched. This position is name as the *phase angle*: $\phi = z\pi/L$ with z being the longitudinal position of the molecule at the time of switching and L the center-to-center distance of two adjacent electrodes. We define the position $\phi = 0$ as in the middle point of two adjacent pairs of electrodes. The synchronous molecule is at the same relative position ϕ_0 each time high voltage configuration is switched. The Stark decelerator will focus on synchronous molecules and capture molecules within a certain range of velocity and space. Such molecules are called phase-stable molecules. When a synchronous molecule passes through a pair of electrode, the kinetic energy lost can be expressed as[57]

$$\Delta K(\phi_0) = \Delta W(\phi_0) = W(\phi_0 + \pi) - W(\phi_0). \quad (1)$$

Here, $W(\phi_0)$ is the Stark potential experienced by the synchronous molecule, expanded using the Fourier series

$$W(\phi_0) = \frac{1}{2}a_0 + \sum_{n=1}^{\infty} a_n \cos\left[n(\phi_0 + \frac{1}{2}\pi)\right]. \quad (2)$$

Substituting Eq. (2) into Eq. (1) yields

$$\Delta K(\phi_0) = 2a_1 \sin(\phi_0). \quad (3)$$

However, continuous variables are required to derive the equations of motion. If the deceleration rate is small compared to the kinetic energy of the molecule, the lost kinetic energy of the synchronous molecule between two successive switch times can be regarded as the result of a continuously acting average force. Within these approximations the average force $\bar{F}$ that acts on the synchronous molecule simply reads

$$\bar{F}(\phi_0) = -\frac{\Delta W(\phi_0)}{L} = -\frac{2a_1}{L}\sin(\phi_0). \quad (4)$$

The motion of the non-synchronous molecule relative to the synchronous molecule in the decelerator can be expressed by

$$\frac{mL}{\pi}\frac{d^2\Delta\phi}{dt^2} + \frac{2a_1}{L}[\sin(\phi_0 + \Delta\phi) - \sin(\phi_0)] = 0. \quad (5)$$

By numerically integrating the above equation, we can obtain the outer contour of the phase stability diagram, know the region where the non-synchronous molecules experience stable oscillations around the synchronous molecules, and understand the longitudinal acceptance of the decelerator so as for the deceleration efficiency.

In our simulation the OH molecule is taken as an example. The ground electronic state of OH is $^2\Pi_{3/2}$. As it enters the decelerator, a Stark energy of $E_{\text{stark}} = \mu\frac{\Omega M_J}{J(J+1)}E$ is generated due to the interaction between the polar molecule and the electric field. Thus, the force exerting on the molecule as it moves is $\boldsymbol{F} = -\nabla E_{\text{stark}}$. Knowing the force, we can calculate the acceleration and solve the equation of motion classically. The Stark deceleration process is modeled with realistic Monte Carlo classical trajectory simulations taking into account the geometry of a Stark decelerator apparatus as well as all externally adjustable parameters such as the deceleration rate, the deceleration potentials, the relative time when to switch on the decelerator and the quantities characterizing the molecular beam.

Results and Discussion. Let us first review the working principle of a Stark decelerator. A conventional Stark decelerator consists of a long array of electrodes extending in the direction of the molecular beam. The electrode pairs are separated by a length L from each other and can be charged to various voltages. A periodic electric potential is realized by charging every even pair of electrodes to opposite high voltages and grounding every odd pair of electrodes. In addition to the traditional Stark deceleration, there is also traveling wave deceleration, which uses a series of ring electrodes charged with time-dependent high voltages, creating a true moving potential to slow molecules. The traveling trap initially moves at the average speed of the molecular beam, then slows its speed to slow down the molecules trapped within. This work is mainly to improve the deceleration efficiency of a conventional Stark decelerator. Next, we compare the ordinary high-voltage configuration with the one proposed here. The corresponding high voltage configuration of the normal switching operation (*normal*) is shown in the left column of Fig. 1. At the beginning, the odd pairs of electrodes are grounded, and the even pairs of electrodes are connected to the positive and negative high voltage. When the molecules climb to the position of the high voltage charged pairs, the electrode voltage is switched to the next configuration as shown in the second row of the left column of Fig. 1. This process is repeated so that the molecules are decelerated. In addition to the normal switching mode, we start with the configuration, i.e., the odd number of electrodes to the ground and the even number of electrodes to the positive high voltage. When the molecule passes through the grounded electrode to the same distance from the electrodes relative to the molecule when the switching sequence started the high-voltage configuration changes to the normal mode. This means that the molecules experience two high-voltage configurations as they pass through one deceleration stage. This operation mode corresponds to the SF mode in the paper of Reens *et al.*,[52] and is named as pg + normal in our paper for consistence (shown in the middle column of Fig. 1). The improved switching sequence pm + normal proposed in this study is similar to the pg + normal mode, except that the grounded electrodes in the second row of the middle column of Fig. 1 are negatively charged (right column in Fig. 1). We find that with suitable combination of the above listed high voltage configurations and careful design of the switching time sequence one can improve the deceleration efficiency by a few factors compared to the existing operation schemes on a small Stark decelerator consisting of only around 150 electrodes. In this study, the efficiency of a Stark decelerator is simply referred to as the ratio of the number of decelerated molecules and the initial number (the initial number of molecules we are modeling is one million). The voltages in each configuration used in our simulations are all ±10 kV.

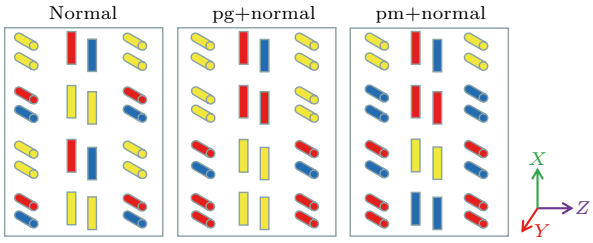

Fig. 1. The diagram shows the electrode voltage configurations of operation scheme of normal, pg + normal and pm + normal, respectively. The colors of yellow, red and blue represent ground, positive-high voltage and negative-high voltage, respectively.

Figure 2 shows one- and three-dimensional simulations of TOF profiles of OH molecules decelerated with the proposed operation schemes. The initial velocity of the OH molecules is 450 m/s, and the the final velocities are 360 m/s, 150 m/s, 50 m/s and 20 m/s for comparison. From the 3D simulation, we found that the number of cold molecules obtained using the improved switching (pm + normal) is on average around one order of magnitude higher than that obtained by using the normal scheme (normal) at the considered final velocities (the number of cold molecules obtained by using the pm + normal method at 150 m/s

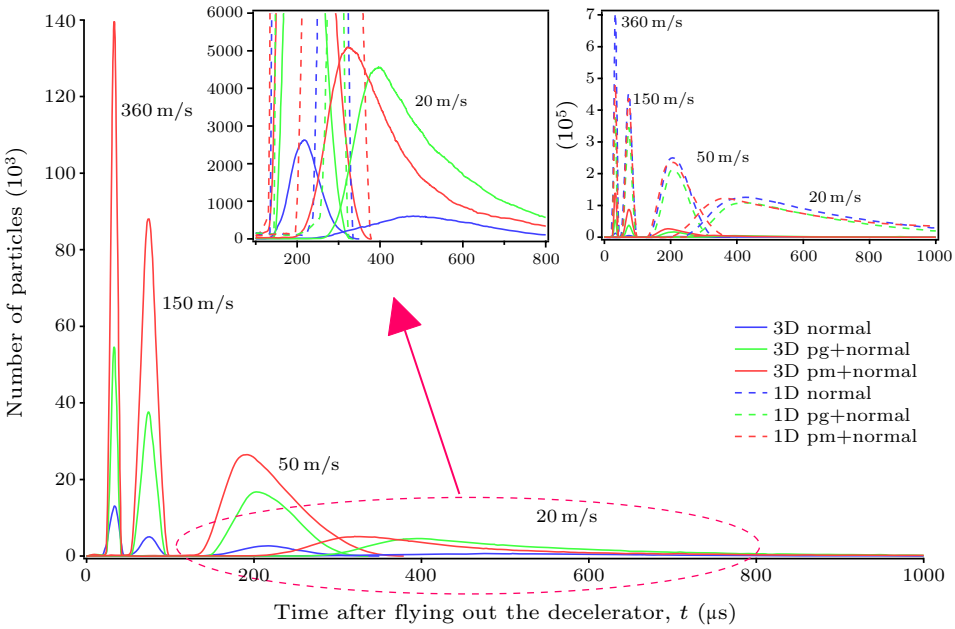

Fig. 2. Time-of-flight profiles of molecules decelerated under normal, pg + normal and pm + normal switching methods. The initial velocities are 450 m/s, and the molecules are slowed down to 360 m/s, 150 m/s, 50 m/s and 20 m/s. The left inset shows zoomed in part of TOF profiles indicated by the pink-dashed circle. The right inset shows the TOF profiles in the ideal one-dimensional case, i.e., all molecules are confined along the longitudinal direction.

is 20 times higher than that obtained by the normal method). The efficiency of obtaining cold molecules using pm + normal is also higher than that using pg + normal. At high final velocity (360 m/s), the efficiency of using pm + normal is more than twice or nearly three times that of pg + normal, but at low final velocity (20 m/s), the efficiency of using pm + normal is only a few tens of percent more than pg + normal. In addition, we also compare the pg + normal with the ordinary switching mode, and find that the efficiency was about 4 times higher at the final speed of 360 m/s, about 7 times higher at the final speed of 150 m/s and 20 m/s, and about 6 times higher at the final speed of 50 m/s. The pg + normal method was briefly discussed in Ref. [52]. In that paper, the authors mentioned two kinds of high-voltage configurations, one is to ground the three electrodes in two adjacent pairs and the fourth one is connected to a positive or negative high voltage, the other is the same as our pg + normal method. Through experiments, they found that the efficiency of the former mode is four times higher than that of the ordinary switch, and the efficiency of pg + normal is higher than that of the former switch which is consistent with our calculation results. In this work we calculate the efficiency of both pg + normal and pm + normal, and finds that pm + normal is the winner. Nevertheless, our improved switching method is still much less efficient than the limiting case of the one-dimensional (with zero lateral motion) simulation. At a high final velocity of 360 m/s, the efficiency of the 3D pm + normal in obtaining cold molecules is only one fifth of that of the one-dimensional conventional switching. At a low final velocity of 20 m/s, the efficiency of using the pm + normal method is about 1/24 of that of a normal switch in the limiting case.

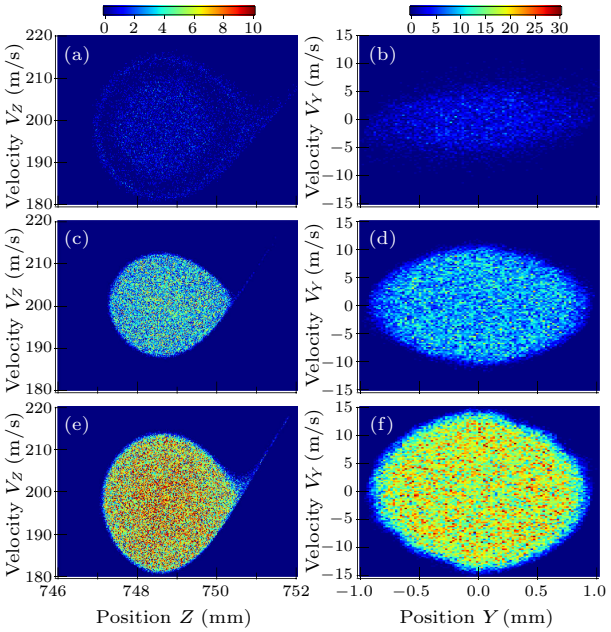

Fig. 3. Phase space diagrams of the Stark slowed molecules from 450 m/s to 200 m/s with different switching options: [(a), (c), (e)] along the Z direction under normal, pg + normal and pm + normal switching modes, respectively; [(b), (d), (f)] along the Y direction under different three modes. The color map represents the number of particles.

In the limiting one-dimensional case, the number of cold molecules obtained is decreasing with final velocities because of the shrinking depth of the effec-

tive trapping potential. In the three-dimensional real world, additional loss appears due to the transverse dynamics of the deceleration process. Molecules are decelerated longitudinally but also bound transversely as they move through the decelerator. It has been shown that the homogeneity of the transverse force plays an important role in determining the deceleration efficiency.[51]

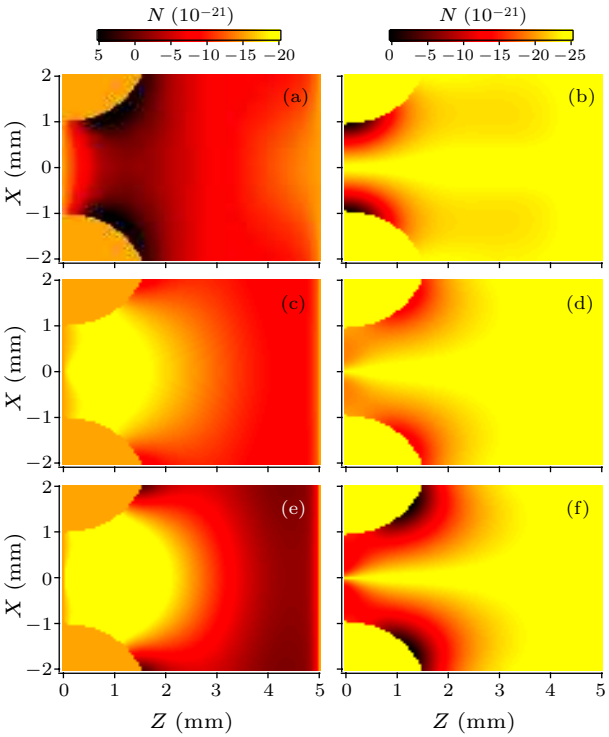

Fig. 4. The force felt by molecules under different three electrode switching conditions: [(a), (c), (e)] the forces exerted by molecules along the Z direction which is responsible for the deceleration in normal, pg + normal and pm + normal modes; [(b), (d), (f)] the averaged forces exerted along the X (or Y) direction in three modes, respectively.

To further understand our simulation results especially the mechanism behind the improvement of the deceleration efficiency under the proposed switching modes. As shown in Fig. 3, we simulate the horizontal and vertical phase-space distribution of molecules when the molecular velocity is slowed from 450 m/s to 200 m/s under three different modes. Figures 3(a), 3(c) and 3(e) show the longitudinal phase-space distribution of molecules under normal, pg + normal and pm + normal modes, respectively. Through the simulation, it is seen that the phase-space volumes for which no stable trajectories exist are shown as an empty area in Fig. 3(a), which indicates the depletion of the particle in this region. This is due to the fact that some molecules cannot be stably slowed down due to the coupling of transverse and longitudinal motion in the decelerator. In Figs. 3(c) and 3(e), the molecules are nicely focused, filling up the whole phase space defined by Eq. (5). Figures 3(b), 3(d) and 3(f) represent the transverse phase-space distributions of molecules operating under three switching schemes, respectively. We can clearly see that pm + normal has better transverse focusing than pg + normal and normal, which manifests as a larger stable region along the velocity direction. This is the reason why the loss number of moving molecules in Fig. 2 decreases successively under the switches modes of normal, pg + normal and pm + normal.

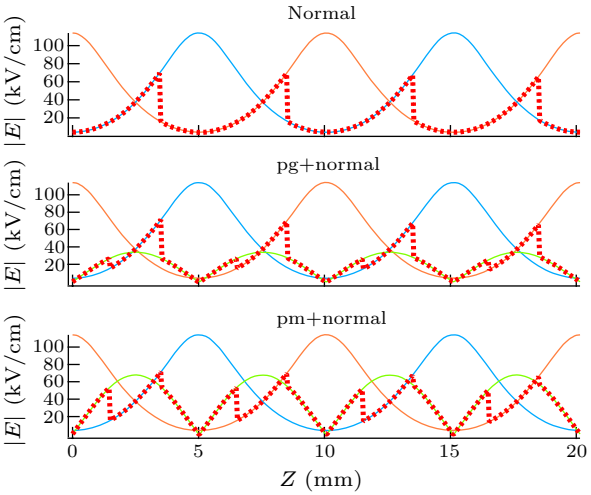

Fig. 5. The diagram showing the electric field changes experienced by an ideal synchronous molecule for three switching modes.

Now let us look at the forces acting on molecules as they move under three switching modes. Figures 4(a), 4(c) and 4(e) represent the longitudinal forces that molecules are subjected to in the XZ plane under normal, pg + normal and pm + normal electrode switchings, respectively. It can be seen that the largest deceleration effect of normal is between the electrode pairs, which is the black area in the figure. However, for pg + normal and pm + normal it is in the middle of the two electrode pairs. The deceleration force is not much stronger in the case of pg + normal and pm + normal compared to normal. Because of this, it is impossible to decelerate molecules to the same amount of finial velocities using pg + normal or pm + normal alone without adding more deceleration units. However, a suitable combination of the pg + normal or pm + normal configuration with the normal can solve this problem. The actual switching sequence is pictured in Fig. 5. It shows the behavior of idealized synchronous molecules propagating along the decelerator shaft at zero transverse velocity under three switching sequences of normal, pg + normal and pm + normal, respectively. The yellow, green and blue line represent the longitudinal Stark potential seen by the molecule moving on the Z axis of the Stark decelerator. The red dotted line in the figure indicates the time of switching. In the normal mode, the high-voltage configuration is switched between a pair of electrodes connected with positive and negative high voltages and a pair of grounded electrodes.

Here, pg + normal is switched in a combination way of normal and pg + normal as shown in the middle part of Fig. 5. Like pg + normal, pm + normal is also switched directly from pm + normal to normal configuration. Figures 4(b), 4(d) and 4(f) represent the transverse forces exerting on the molecule in the Y direction. The area which contains appreciable transverse forces is the largest for the pm + normal case, medium for the pg + normal case and the smallest for the normal case. This is exactly the reason responsible for the different deceleration efficiencies obtained from the numerical simulations.

In summary, we have presented a new type of operation methods on the basis of a traditional Stark decelerator. With the help of trajectory calculation, we find that the proposed method can better focus the decelerating molecules compared with other ways for a conventional Stark decelerator without increasing the length of it. A larger number of cold molecules can be obtained, which greatly improves the efficiency and extends the regime of the applications of a Stark decelerator. The proposed methods, though require some modifications of the electronics for a Stark decelerator, are expected to be widely applied in the cold molecule community.

References

[1] Carr L D, DeMille D, Krems R V and Ye J 2009 *New J. Phys.* **11** 055049
[2] Tomza M, Jachymski K, Gerritsma R, Negretti A, Calarco T, Idziaszek Z and Julienne P S 2019 *Rev. Mod. Phys.* **91** 035001
[3] Wall T E 2016 *J. Phys. B* **49** 243001
[4] Safronova M S, Budker D, DeMille D, Kimball D F J, Derevianko A and Clark C W 2018 *Rev. Mod. Phys.* **90** 025008
[5] Chupp T E, Fierlinger P, Ramsey-Musolf M J and Singh J T 2019 *Rev. Mod. Phys.* **91** 015001
[6] Cairncross W B and Ye J 2019 *Nat. Rev. Phys.* **1** 510
[7] Lin Y, Leibrandt D R, Leibfried D and Chou C W 2020 *Nature* **581** 273
[8] Albert V V, Covey J P and Preskill J 2020 *Phys. Rev. X* **10** 031050
[9] Phillips W D 1998 *Rev. Mod. Phys.* **70** 721
[10] Liang Z T, Lv Q X, Zhang S C, Wu W T, Du Y X, Yan H and Zhu S L 2019 *Chin. Phys. Lett.* **36** 080301
[11] Yuan J, Ma Y, Li R, Ma H, Zhang Y, Ye D, Shen Z, Yan T M, Wang X, Weidemüller M and Jiang Y 2020 *Chin. Phys. Lett.* **37** 053201
[12] Wang K P, Zhuang J, He X D, Guo R J, Sheng C, Xu P, Liu M, Wang J and Zhan M S 2020 *Chin. Phys. Lett.* **37** 044209
[13] Zhou P P, Chen S L, Liang S Y, Sun W and Gao K L 2020 *Chin. Phys. Lett.* **37** 093701
[14] Chen S L, Zhou P P, Liang S Y, Sun W, Sun H Y, Huang Y, Guan H and Gao K L 2020 *Chin. Phys. Lett.* **37** 073201
[15] Ubachs W, Bagdonaite J, Salumbides E J, Murphy M T and Kaper L 2016 *Rev. Mod. Phys.* **88** 021003
[16] Bethlem H L, Berden G and Meijer G 1999 *Phys. Rev. Lett.* **83** 1558
[17] Schnell M and Meijer G 2009 *Angew. Chem. Int. Ed.* **48** 6010
[18] van de Meerakker S Y T, Bethlem H L, Vanhaecke N and Meijer G 2012 *Chem. Rev.* **112** 4828
[19] Haas D, Scherb S, Dongdong Z and Willitsch S 2017 *EPJ. Tech. Instrum.* **4** 6
[20] Fu G B, Deng L Z and Yin J P 2008 *Chin. Phys. Lett.* **25** 923
[21] Deng L Z, Fu G B and Yin J P 2009 *Chin. Phys. B* **18** 149
[22] Yin Y L, Xia Y and Yin J P 2006 *Chin. Phys. Lett.* **23** 2737
[23] Vanhaecke N, Meier U, Andrist M, Meier B H and Merkt F 2007 *Phys. Rev. A* **75** 031402
[24] Narevicius E, Parthey C G, Libson A, Riedel M F, Even U and Raizen M G 2007 *New J. Phys.* **9** 96
[25] Hogan S D, Motsch M and Merkt F 2011 *Phys. Chem. Chem. Phys.* **13** 18705
[26] Lavert-Ofir E *et al.* 2011 *Phys. Chem. Chem. Phys.* **13** 18948
[27] Narevicius E and Raizen M G 2012 *Chem. Rev.* **112** 4879
[28] Damjanović T *et al.* 2021 *New J. Phys.* **23** 105006
[29] Damjanović T, Willitsch S, Vanhaecke N, Haak H, Meijer G, Cromiéres J P and Zhang D 2021 *New J. Phys.* **23** 105007
[30] Hutzler N R, Lu H I and Doyle J M 2012 *Chem. Rev.* **112** 4803
[31] Truppe S *et al.* 2018 *J. Mod. Opt.* **65** 648
[32] Tarbutt M R 2018 *Contemp. Phys.* **59** 356
[33] Yin Y, Xu S, Xia M, Xia Y and Yin J 2018 *Phys. Rev. A* **97** 043403
[34] Yan K, Wei B, Yin Y, Xu S, Xu L, Xia M, Gu R, Xia Y and Yin J 2020 *New J. Phys.* **22** 033003
[35] Jones K M, Tiesinga E, Lett P D and Julienne P S 2006 *Rev. Mod. Phys.* **78** 483
[36] Ulmanis J, Deiglmayr J, Repp M, Wester R and Weidemüller M 2012 *Chem. Rev.* **112** 4890
[37] Köhler T, Góral K and Julienne P S 2006 *Rev. Mod. Phys.* **78** 1311
[38] Chin C, Grimm R, Julienne P and Tiesinga E 2010 *Rev. Mod. Phys.* **82** 1225
[39] Yan X C, Sun D L, Wang L, Min J, Peng S G and Jiang K J 2021 *Chin. Phys. Lett.* **38** 056701
[40] Guo G F, Bao X X, Ta N L and Gu H Q 2021 *Chin. Phys. Lett.* **38** 040302
[41] He X, Wang K, Zhuang J, Xu P, Gao X, Guo R, Sheng C, Liu M, Wang J, Li J, Shlyapnikov G V and Zhan M 2020 *Science* **370** 331
[42] Cheuk L W, De An R L, Augenbraun B L, Bao Y, Burchesky S, Ketterle W and Doyle J M 2018 *Phys. Rev. Lett.* **121** 083201
[43] Enomoto K, Kasa K, Kitagawa M and Takahashi Y 2008 *Phys. Rev. Lett.* **101** 203201
[44] Bloch I, Dalibard J and Zwerger W 2008 *Rev. Mod. Phys.* **80** 885
[45] Wang Q, Hou S, Xu L and Yin J 2016 *Phys. Chem. Chem. Phys.* **18** 5432
[46] Bochinski J R, Hudson E R, Lewandowski H J and Ye J 2004 *Phys. Rev. A* **70** 043410
[47] van de Meerakker S Y T, Vanhaecke N, Bethlem H L and Meijer G 2005 *Phys. Rev. A* **71** 053409
[48] Gilijamse J J, Küpper J, Hoekstra S, Vanhaecke N, van de Meerakker S Y T and Meijer G 2006 *Phys. Rev. A* **73** 063410
[49] van de Meerakker S Y T, Vanhaecke N, Bethlem H L and Meijer G 2006 *Phys. Rev. A* **73** 023401
[50] Scharfenberg L, Haak H, Meijer G and van de Meerakker S Y T 2009 *Phys. Rev. A* **79** 023410
[51] Zhang D, Meijer G and Vanhaecke N 2016 *Phys. Rev. A* **93** 023408
[52] Reens D, Wu H, Aeppli A, McAuliffe A, Wcisło P, Langen T and Ye J 2020 *Phys. Rev. Res.* **2** 033095
[53] Hudson E R, Bochinski J R, Lewandowski H J, Sawyer B C and Ye J 2004 *Eur. Phys. J. D* **31** 351
[54] Tarbutt M R *et al.* 2004 *Phys. Rev. Lett.* **92** 173002
[55] van de Meerakker S Y T, Smeets P H M, Vanhaecke N, Jongma R T and Meijer G 2005 *Phys. Rev. Lett.* **94** 023004
[56] Sawyer B C, Stuhl B K, Lev B L, Ye J and Hudson E R 2008 *Eur. Phys. J. D* **48** 197
[57] van der Meerakker S Y T 2006 *PhD Dissertation* (Radboud Universiteit)